

Stress transmission through three-dimensional ordered granular arrays

Nathan W. Mueggenburg, Heinrich M. Jaeger, and Sidney R. Nagel

The James Franck Institute and Department of Physics, The University of Chicago, 5640 South Ellis Avenue, Chicago, Illinois 60637

(Received 24 April 2002; published 23 September 2002)

We measure the local contact forces at both the top and bottom boundaries of three-dimensional face-centered-cubic and hexagonal-close-packed granular crystals in response to an external force applied to a small area at the top surface. Depending on the crystal structure, we find markedly different results which can be understood in terms of force balance considerations in the specific geometry of the crystal. Small amounts of disorder are found to create additional structure at both the top and bottom surfaces.

DOI: 10.1103/PhysRevE.66.031304

PACS number(s): 81.05.Rm, 83.80.Fg, 45.70.Cc

I. INTRODUCTION

In a static granular bead pack all of the forces on a particle, due to the contacts from its neighbors and due to gravity, must be in perfect balance; there can be no net force on any particle. Moreover, in the limit of hard particles, no particle distortion is allowed leading several investigators to question whether elastoplasticity theory can be used in this hard-sphere limit to describe the mechanical properties of an amorphous granular material [1–4]. Others suggest that elastic theory is capable of producing the observed experimental results [5,6]. The presence of disorder makes an exact calculation of the contact forces in such a material impossible. On the other hand, it should be possible to calculate the forces exactly in a perfect crystal [7]. However, because macroscopic grains do not spontaneously crystallize, it has been difficult to create large defect-free granular crystals [8–11] on which to perform an experiment to see how the forces are transmitted. In addition, there will always be small imperfections or asperities in the particles themselves and slight variations in the diameters of the grains. Although we cannot completely avoid disorder of this latter kind, we have found an efficient method of constructing essentially perfect crystals with few, if any, defects in the particle positions [12]. With such crystals, one would hope that the presence of a small disorder from the variation of the individual particle shapes and sizes could be treated as a perturbation about the perfect crystalline response.

Previously, there have been experimental studies on the statistical properties of the local contact forces in granular packs. In particular, the distribution of normal forces, $P(F)$, between the particles and the container walls was measured in a variety of situations [12–15]. In most of those studies, a piston pressed down on the entire top surface of the granular material. The surprising result was that the entire form of $P(F)$ (a large value near $F=0$, a small peak [or plateau] with a maximum near the average force and an exponential tail at large forces) was robust and did not depend on whether the granular medium was amorphous or crystalline or whether the particles were smooth or rough [12]. The question is thus raised as to what aspects of the force propagation in a granular material are affected by preparation and the underlying crystal or amorphous structure.

Several experiments have studied the response (i.e., the Green's function) to a localized external force at the top sur-

face of a granular medium. The different studies found somewhat contradictory results. DaSilva and Rajchenbach [16] studied a system consisting of a special two-dimensional packing of photoelastic rectangular bricks. They measured the contact forces between particles as a function of position and found that the contact forces had a maximum centered below the position of the applied perturbation and that on either side the forces decreased in magnitude. The width of this peak in the forces grew as the square root of the depth below the surface. This result is consistent with models predicting a diffusive propagation of the forces such as the q model proposed by Coppersmith and co-workers [17,18]. Other studies have focused on the response to a localized external force in amorphous packings of spheres. Reydellet and Clément found that the response at the bottom of a three-dimensional pack had a central maximum of approximately Lorentzian shape with a width that grew linearly with the depth of the pack [19]. Similar behavior was found in two-dimensional samples studied by Geng *et al.* [20]. This linear increase of the width with depth is consistent with elastic theories [5,6]. The work by Geng *et al.* also suggests a strong effect due to the spatial ordering of the particles resulting in a central minimum of the response forces in ordered packings. Thus there is a need to study the propagation of forces from a localized perturbation in a nearly perfectly ordered crystalline array of particles in order to investigate how the underlying order (or disorder) of the lattice influences the force propagation.

Bouchaud *et al.* have proposed a model in which forces propagate in straight lines until encountering a defect where they are split, and they have shown that this model leads to a central force minimum for small depths and to elasticlike behavior for large pack depths [21]. The straight-line propagation of forces (resulting from the hyperbolic model of Cates *et al.* [22]) and the splitting of forces can be viewed in a geometrical framework based upon the contact orientations of neighboring beads. From this viewpoint crystalline packings allow for the control of these contact orientations and the resulting splitting. In particular, the hexagonal-close-packed (hcp) crystal structure is such that forces are required to split at nearly every layer as they travel downward through the pack. By looking at the response of an hcp crystal to a localized force it is possible to explore the consequences of multiple splittings in comparison with the predictions of the forcechain splitting model.

In this paper we present an experimental investigation of the response to a localized external force in three-dimensional nearly perfect hcp and face-centered-cubic (fcc) crystals. We measure the resulting contact forces at both the top and bottom surfaces of the crystal, and investigate how the pattern of forces depends on the crystal structure and the depth of the pack. We determine that in the regime of highly ordered granular packs, the crystal structure plays a dominant role in determining the average pattern of response forces at the bottom surface. These patterns can be viewed as a consequence of force balance in the specific geometry of the crystal. We also consider the effect of small amounts of disorder in these crystals and show that they modify the pattern of forces on the bottom surface in a nontrivial manner and scatter forces back upwards through the pack to the top surface.

II. EXPERIMENTAL METHODS

We created large nearly perfect hcp and fcc granular crystals of 3.06 ± 0.04 mm diameter soda lime glass spheres. These crystals of approximately 53-bead-diameters on a side were contained within an acrylic cylinder with a triangular cross section designed to be commensurate with the hcp crystal structure. The crystals were created as individual layers of triangular order in the manner described in Ref. [12]. In this way the position of each individual bead was viewed and corrected if necessary as the crystal was constructed, so that the resulting crystal would have very few defects (estimated to be less than ten beads significantly out of place for a crystal of approximately 50 000 beads). Furthermore, the stacking order of the planes was controlled in order to achieve three-dimensional fcc and hcp crystals.

After building such a crystal we applied an external force to a localized region at the center of the top of the crystal either by using a slowly applied steady force of approximately 100 lb or by using a quick impulse force. When using the slowly applied force it was necessary to apply the force over a region approximately six beads in diameter. Attempts to apply the force to a smaller region resulted in significant bead movement. When using the quick impulse force it was possible to apply the force to a smaller area of approximately two beads in diameter. For the purpose of comparison experiments were also carried out with the quick impulse force applied to the large six-bead-diameter region.

We used a carbon paper technique to measure the forces in response to the external forces [12,13,17,23]. A piece of carbon paper and a piece of white paper [24] were placed on the top and bottom of the crystal. As the force was applied, individual beads pressed into the carbon paper and left marks on the white paper. The size and darkness of the resulting marks were related to the normal force on the corresponding beads. When using the slowly applied force, we calibrated the force versus darkness response as explained in Ref. [12]. The positions of the carbon marks were matched to a triangular lattice and the forces for each lattice point were averaged over approximately ten experimental runs. It is important to note that individual runs vary significantly, but that the average over many runs remains highly reproducible. In

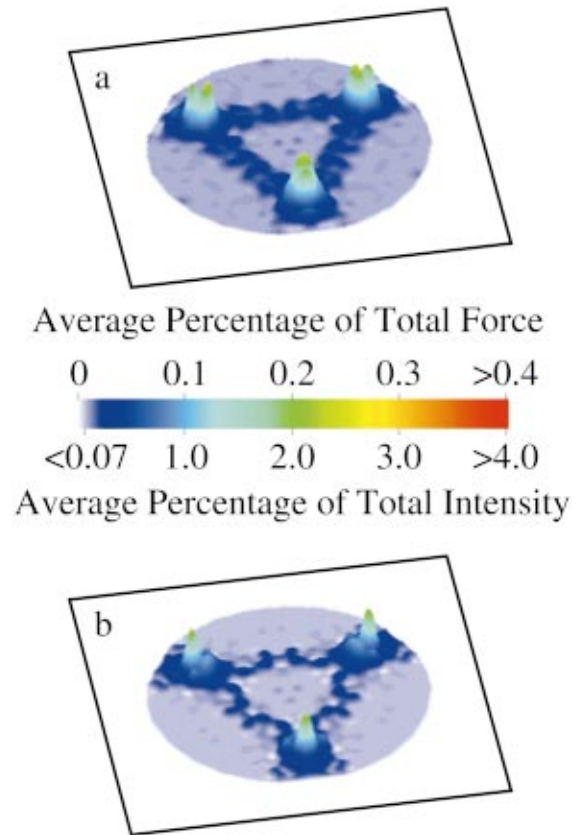


FIG. 1. (Color) A comparison of the pattern of calibrated forces in response to a slowly applied force to the pattern of intensities in response to a quick impulse force. (a) The pattern of calibrated forces at the bottom surface of a 19 layer fcc crystal in response to a slowly applied force over an area six beads in diameter at the top surface. (b) The pattern of intensities of carbon marks in response to a quick impulse force applied to the same crystal structure over the same area. Both pictures represent an average over ten experimental runs and an average over crystal symmetries.

order to improve statistics, the locally measured forces were also averaged over symmetries of the crystal (one reflection and two rotations).

Note that the analysis technique must be carried out carefully so as not to introduce error from the averaging over many files, and crystal symmetries. If the centers of the images are not determined accurately, then lattice positions from file to file will not match up exactly and will result in a small degree of broadening of any features. We estimate this broadening to be significantly less than one-bead diameter for each of the regions of large force.

When using the quick impulse, we calibrate the measured forces by comparing them with those obtained with an identical setup using the slowly applied force described above. We compared the patterns of carbon marks left by the two methods and found no qualitative difference. Figure 1(a) shows the pattern of calibrated forces at the bottom of a 19 layer fcc crystal in response to a slowly applied force at the top surface over a region six beads in diameter. The calibration maps points of zero intensity to a small but nonzero force which results in a nonzero background. Figure 1(b)

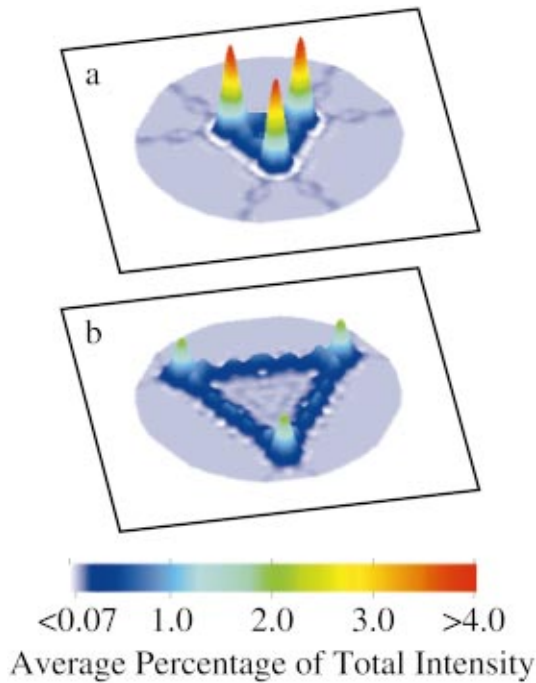


FIG. 2. (Color) Intensity patterns at the bottom surface of fcc crystals (a) 9 and (b) 19 layers in depth in response to a quick impulse force applied to a two-bead-diameter region at the top surface.

shows the pattern of intensities of carbon marks at the bottom of a similar crystal in response to a quick impulse force applied to the same area. The color scale of intensity has been shifted by a factor of ten and a minimum value used to match the previous pattern of forces. Using this shift in color scale intensity we map the two different measurements onto one another and obtain a calibration for the quick impulse.

III. RESULTS

A. fcc crystals

For fcc crystals we found a characteristic response pattern at the bottom surface which is qualitatively independent of the type of force applied. Figure 2 shows the patterns of intensities at the bottom of fcc crystals, 9 and 19 layers in depth, in response to a quick impulse force applied to an area two beads in diameter at the center of the top surface of the crystal averaged over approximately ten experimental runs and averaged over crystal symmetries. We find three regions of large force, arranged in a triangular pattern. The size of this triangle increases with the depth of the crystal. The size of the three regions of large force are comparable to the size of the region over which the force was applied. In addition to the three regions of large force, there appear fainter but still significant regions of force along the lines connecting these three regions.

Figures 3(a) and 3(b) show cross sections of the intensity versus position across the triangular pattern at the bottom surface of 9 and 19 layer fcc crystals. As depicted in the inset of Fig. 3(a) the cross section proceeds across the edge of the triangular pattern, corresponding to a small peak, through the

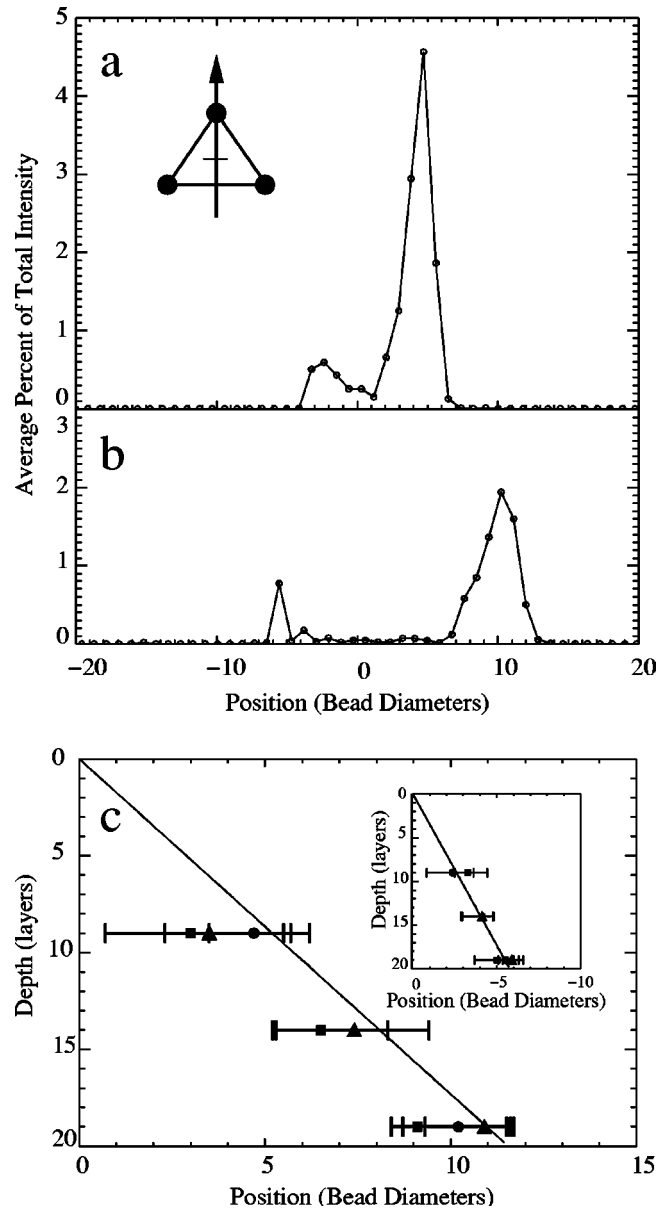


FIG. 3. Intensity as a function of position at the bottom of fcc crystals (a) 9 and (b) 19 layers in depth in response to a quick impulse force applied to an area two beads in diameter at the top of the pack. The cross section was taken through the triangular pattern of intensity as shown in the inset. (c) The position of main intensity peaks as a function of the depth of the pack in response to (circles) a quick impulse force over a small area, (triangles) a quick impulse force over a large area, and (squares) a slowly applied force over a large area. Error bars represent the full width at half the maximum value of the peaks. The black line indicates a slope of 35.3° with respect to the vertical which corresponds to an angle specific to the geometry of the fcc crystal. The inset shows the position of the smaller peaks corresponding to the edge of the triangular pattern with a line representing an angle of 19.5° .

center of the pattern (position=0) with small intensities, and across the region of large force, corresponding to a large peak. The position of the large peaks as a function of the depth of the crystal are indicated in Fig. 3(c), with the error bars corresponding to the full width at half maximum of the

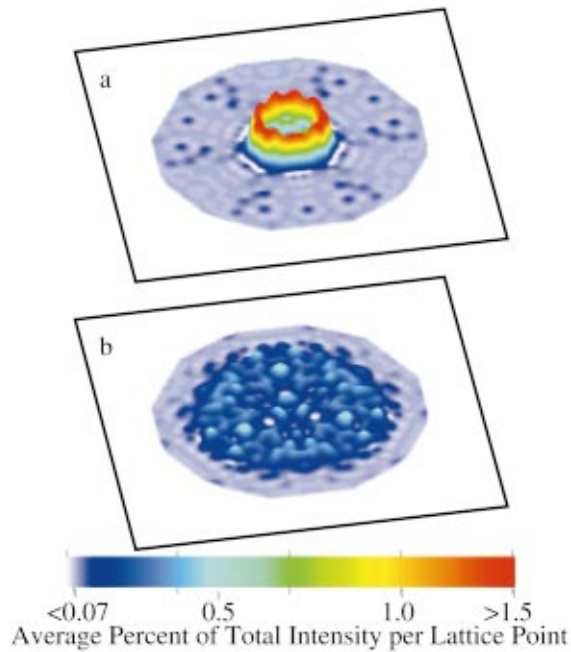


FIG. 4. (Color) Intensity patterns at the bottom of hcp crystals (a) 9 and (b) 25 layers in depth in response to a quick impulse force over an area two beads in diameter at the top surface of the crystal. In order to show the structure more clearly, the color scale has been scaled relative to that in Figs. 1 and 2 with the low intensity cutoff color remaining the same.

peaks, which can in some cases be seen to be significantly skewed. Additional data points are included in Fig. 3(c) corresponding to experimental runs with a quick impulse applied to a large area and to runs with a slowly applied force over a large area. The sloped line indicates an angle of 35.3° , which corresponds to the angle down the edge of a tetrahedron. The regions of large force are found to lie just inside of this angle as explained in Sec. IV. The inset of Fig. 3(c) shows the position of the small peaks corresponding to the edge of the triangular patterns as a function of the depth of the crystal packing. The solid line shows an angle of 19.5° with respect to the vertical, which corresponds to the angle down the face of a tetrahedron.

B. hcp crystals

In contrast to the triangular patterns found for fcc crystals, hcp crystals show rings of large force at the bottom surface in response to a localized force at the top surface. Figure 4 shows the intensity patterns at the bottom surfaces of hcp crystals 9 and 25 layers in depth in response to a quick impulse force applied to an area two beads in diameter at the top surface averaged over approximately ten experimental runs and averaged over crystal symmetries. As the depth of the pack increases the radius of the ring increases, and interior fills in. Figures 5(a) and 5(b) show the radial distribution of intensity for hcp crystals of 9 and 25 layers in depth in response to a quick impulse force over a small area. Figure 5(c) shows the position of the peaks in intensity as a function of the depth of the pack with the error bars corresponding to the width of the peak at half of the maximum value. For hcp

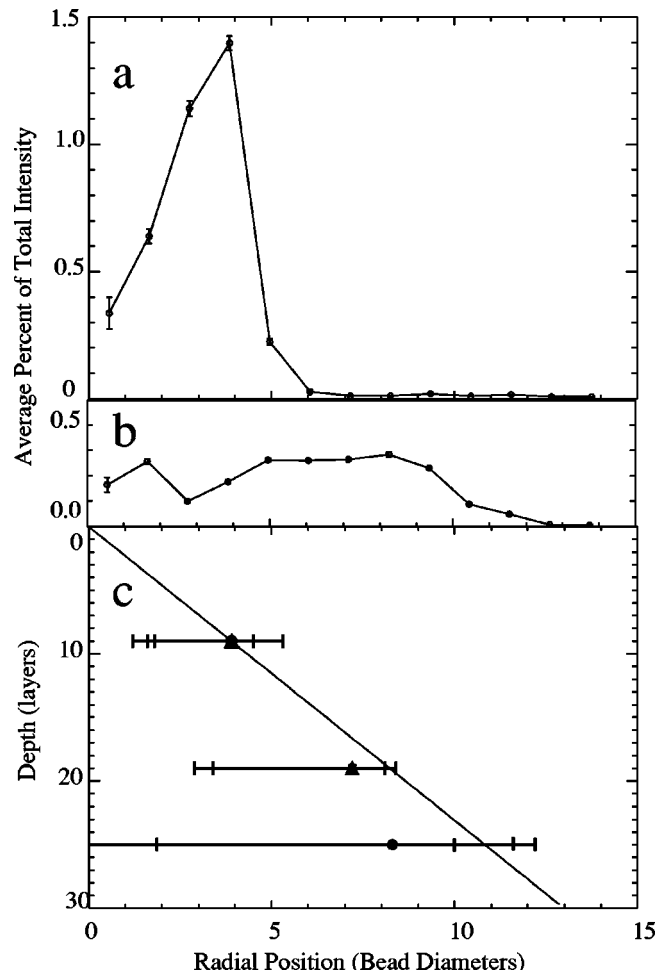


FIG. 5. Radial distribution of intensity at the bottom of hcp crystals (a) 9 and (b) 25 layers in depth in response to a quick impulse force applied to a small area at the top surface. The position of the peaks as a function of the depth of the pack are shown in (c) as circles with error bars representing the full width at half of the maximum value of the peak. As the interior of the ring is nearly uniform no lower bound is shown for the 25 layer crystal. The triangular data points indicate similar peaks in response to a quick impulse force over a large area, and the square data points correspond to a slowly applied force over a large area. The solid line corresponds to an angle of 27.4° with respect to the vertical which is the average of two angles specific to an hcp crystal structure as explained in the text.

crystals 25 layers in depth the intensity is nearly uniform and thus no lower bound is shown. Additional data points are included corresponding to experimental runs with a quick impulse applied to a large area and to runs with a slowly applied force over a large area. The sloped line indicates an angle of 27.4° which is the average of the angles down the edge and the face of a tetrahedron. The peaks in intensity and force are found to lie just inside of this angle as explained in Sec. IV.

C. Amorphous packings

The response of an amorphous pack shows a broad central peak centered below the applied force. The carbon paper

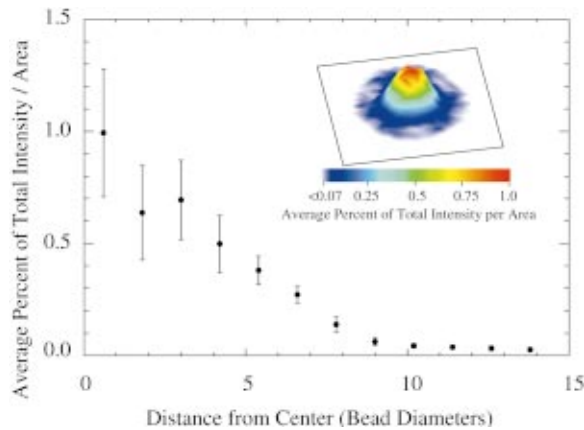


FIG. 6. (Color) Radial distribution of intensity at the bottom of amorphous packings 1.0 in. depth in response to a quick impulse force applied to a large area at the top surface averaged over ten experimental runs. Error bars represent the standard deviation across the multiple experimental realizations.

technique is limited in its usefulness on amorphous packings as a localized force large enough to leave carbon marks will often result in significant penetration of the piston into the pack with consequent movement of the grains. As such, we were only able to explore the response of amorphous packings to the quick impulse force applied to a large six-bead-diameter region. Figure 6 shows the dependence of force on distance from the center of the broad central peak, averaged over ten experimental runs and over azimuthal angle. Our data on the width of this central maximum are consistent with a square-root growth with depth as seen in a two-dimensional packing of bricks by DaSilva and Rajchenbach [16], but are also within error of a linear growth as seen by Reydellet and Clément [19] in three-dimensional packings. The task of distinguishing between such behaviors is better suited to other experimental techniques.

D. Top surface

In addition to measuring the response at the bottom of the crystal packs, we also used the carbon paper technique to measure the response in systems at the top of the pack. Figure 7 shows surface plots for the average intensity of the carbon dots as a function of position at the top surface of the crystal in response to a quick impulse applied to an area two beads in diameter. Both fcc and hcp crystals show a characteristic sixfold spoke pattern, which does not depend significantly on the depth of the crystal. The magnitude of the average intensity in these spokes is approximately ten times less than the intensity in the regions of large force on the bottom surface, but they are still significantly stronger than the surrounding background. The spokes extend all the way to the edge of the analysis region (15-bead diameters in radius) without a significant decrease in intensity.

IV. GEOMETRICAL INTERPRETATION

A. fcc geometry

Many aspects of the patterns of force or intensity seen in the crystalline packings (Figs. 1, 2, 4, and 7) can be ex-

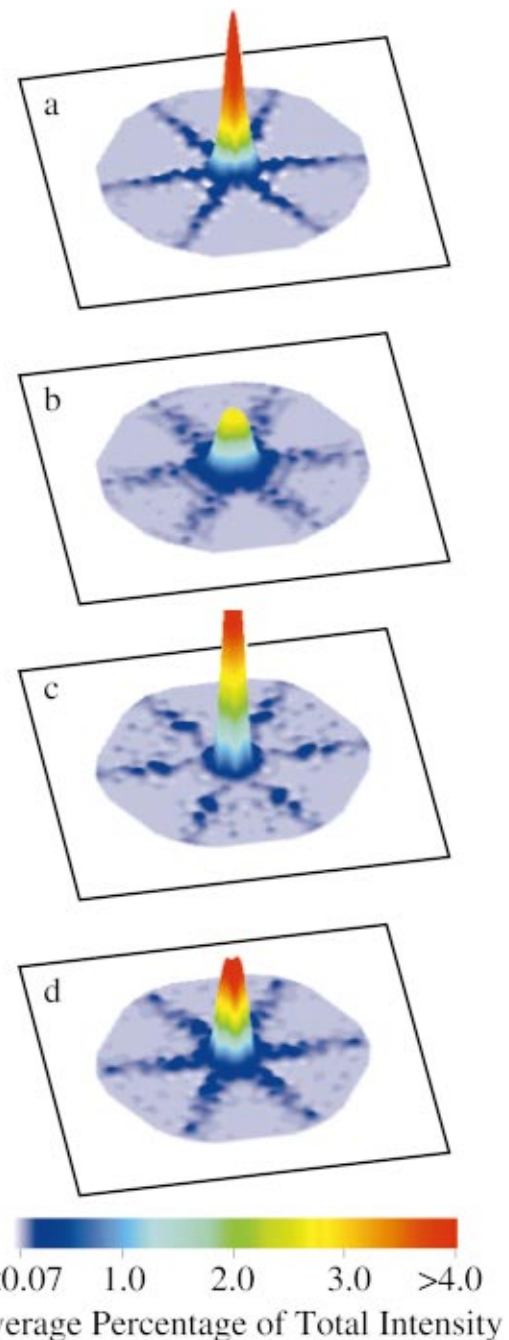


FIG. 7. (Color) Intensity patterns at the top surface of (a) a 3 layer hcp crystal, (b) a 9 layer hcp crystal, (c) a 9 layer fcc crystal, and (d) a 19 layer fcc crystal in response to a quick impulse force applied to a small area in the center of these images. Each image is averaged over approximately ten experimental runs and averaged over crystal symmetries. The sixfold spoke pattern is present in both types of crystal packings and does not depend on the depth of the packing.

plained through force balance in the specific geometry of the crystals. Our fcc crystals were oriented with the 111 plane horizontal, so that they consisted of a stack of triangularly ordered planes. This is equivalent to a typical cannon ball piling. In an fcc crystal the stacking order from plane to plane is such that every third layer lies on top of the first.

This results in straight lines of contacts between beads running diagonally down through the pack.

Figure 8 shows the geometry of a piece of a perfect fcc crystal. If a downward force is applied to the bead at the top of this pyramidal pile, then the force is transmitted to the three beads below it in the second layer. Essentially, the bead at the top of the pyramid is supported by a tripod, with three lines of beads stretching downward through the pack. Only the beads in this tripod will feel a force in response to the force on the top bead. All other beads inside and outside of the pyramid are shielded from that force. Thus, at the bottom of the crystal there are only three beads which feel any force. These beads are arranged in a triangular pattern with the size of the triangle proportional to the depth of the pack. The legs of the tripod in the fcc crystal are at an angle of 35.3° with respect to the vertical. Given this angle the position of the beads which feel the applied force is determined. The solid line in Fig. 3(c) shows the predicted angle of 35.3° .

B. Disorder

If there is a small amount of disorder in the crystal, then the positions of the beads within the tripod legs will not be perfectly aligned. Thus, in order to balance the forces vectorally, there must be some force scattered off the tripod. For a small degree of disorder, the majority of the force will still be transmitted along the tripod legs, with a small amount scattered to one or more additional neighboring beads. Figure 8(c) represents an fcc crystal with one point of disorder in the second layer. Most of the force is transmitted along the tripod legs, but a small amount is scattered along the blue line. If there is no further disorder, then this scattered force will propagate along its own line of beads all of the way to the bottom of the pack, and arrive at the bottom surface along one of the lines connecting the three ends of the tripod legs, as shown in Fig. 8(d). Using this as a model for the effect of one point of disorder we find that, when considering a small degree of disorder throughout the system, the majority of the force is transmitted along the tripod legs, with a small amount scattered down the sides of the pyramid and arriving at the bottom surface along the edges of the triangle formed by the tripod legs. Figure 8(e) shows the first-order effect of scattering within an fcc crystal. The red lines represent strong force, and the blue lines represent weaker forces resulting from first-order scattering. The pattern of forces at the bottom of the crystal, shown in Fig. 8(f) is seen in the images in Figs. 1 and 2.

Disorder can also explain the appearance of the regions of large force at angles slightly smaller than 35.3° as seen in Fig. 3(c) as scattered forces arriving preferentially inside the triangular pattern will skew the regions of large force towards the inside of the pyramid. To first order, no force exists outside of the pyramid.

If at points of disorder the force scatters to beads in plane rather than to the plane below, then without additional scattering the scattered force propagates straight outward to the sides of the container. For nonclose-packed systems, in which in-plane beads are not in contact, it is also possible for the forces to scatter upwards through the pack. This would

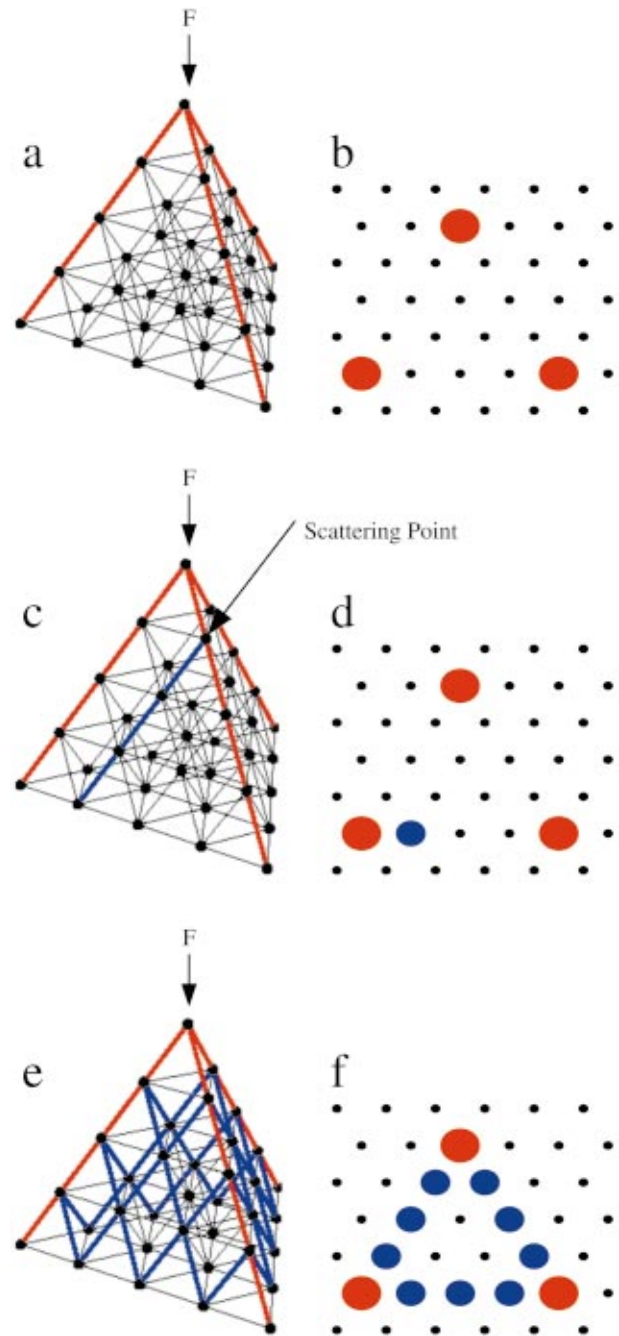


FIG. 8. (Color) Geometric interpretation of the response to a point force in an fcc crystal. (a) In a perfect fcc crystal the force at the top of the pyramid is balanced by a tripod. (b) At the bottom layer only three beads support force. (c) One point of disorder along a tripod leg results in a scattering of a small amount of force off the tripod leg. In this case the force is shown being scattered downward. (d) This scattered force propagates downward to the bottom surface to one of the lines connecting the regions of large force. (e) Averaging over all possible points of single downward scattering events, the scattered forces are contained on the faces of the pyramidal structure. (f) The scattered forces arrive at the bottom layer arranged along the lines connecting the nonscattered forces.

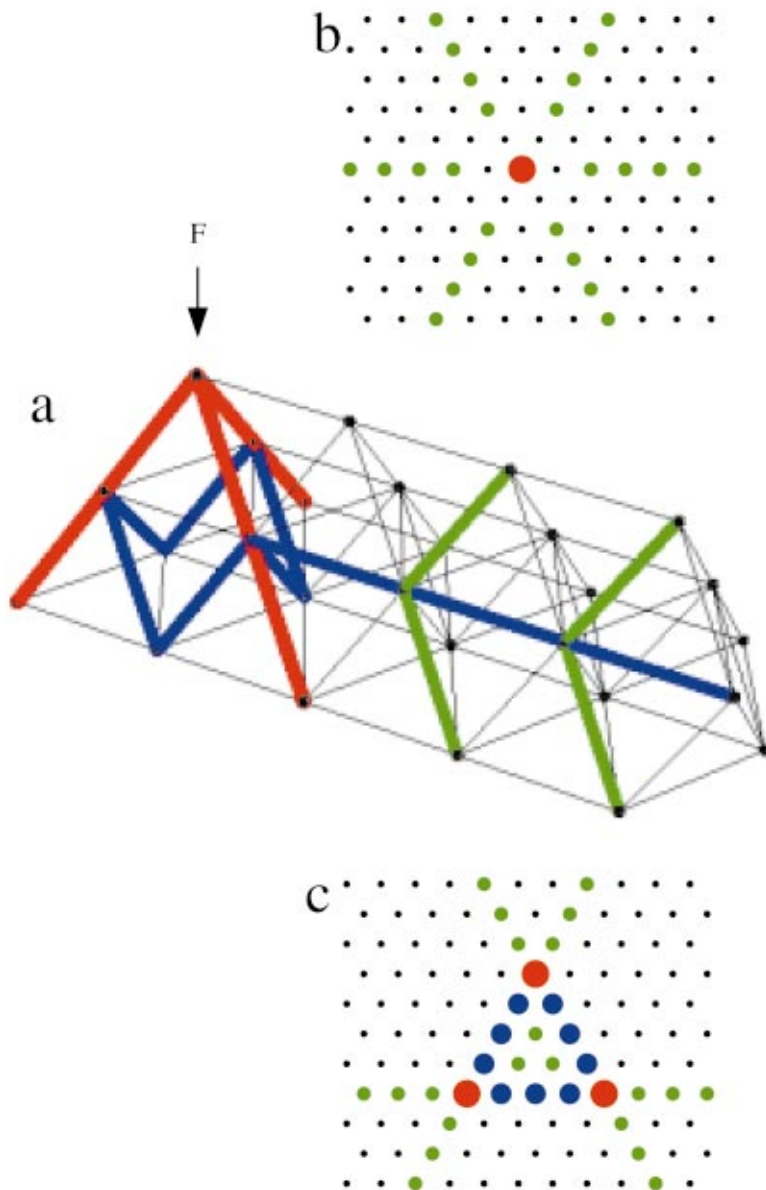


FIG. 9. (Color) (a) Schematic diagram of an fcc crystal showing second-order scattering. The red lines represent large unscattered forces. Blue lines correspond to first-order scattering, both downward and in plane, and green lines represent some of the second-order scattering. Also shown are the patterns at the (b) top and (c) bottom surfaces of a five layer fcc crystal due to second-order scattering.

produce a spokelike structure, but the length of the spokes would be expected to depend on the depth of the pack which is not seen experimentally.

The second-order effect of disorder on the transmission of forces is depicted in Fig. 9. Figure 9(a) shows a piece of a three layer fcc crystal. The red lines represent the strong forces along the tripod discussed earlier. The blue lines are the result of first-order scattering with both in plane and downward scattering shown. The green lines represent some of the scattering from the scattered forces, or second-order scattering. Of interest is the scattering from the in-plane forces. These forces can scatter upwards, downwards, or in plane through the pack. Figure 9(b) shows the forces at the top surface of a five layer deep fcc crystal, where second-order scattering produces a sixfold spoke pattern extending radially outward from the center after a one-bead gap. These spokes extend outward to the edge of the system and do not depend on the depth of the crystal. Similar experimental spoke patterns are shown in Fig. 7. Figure 9(c) shows the

pattern of forces at the bottom surface of the crystal where the effect of second-order scattering is to fill in the triangle with very weak forces and extend the edges of the triangle beyond the vertices. For small amounts of disorder the magnitude of the forces from second-order scattering is much smaller than those previously discussed. Nevertheless, Fig. 2(a) shows faint forces along the lines of the triangle edges beyond the vertices.

C. hcp Geometry

The hcp crystals that we studied are also oriented so as to consist of stacked planes of triangular order. Unlike the fcc crystals the stacking of the planes is such that every other plane lies directly above the first. The top two layers of an hcp crystal and fcc crystal are identical, and the force transmission will be the same. However, the difference in position of the beads in the subsequent layers causes the force transmission to be markedly different. In an hcp crystal there are

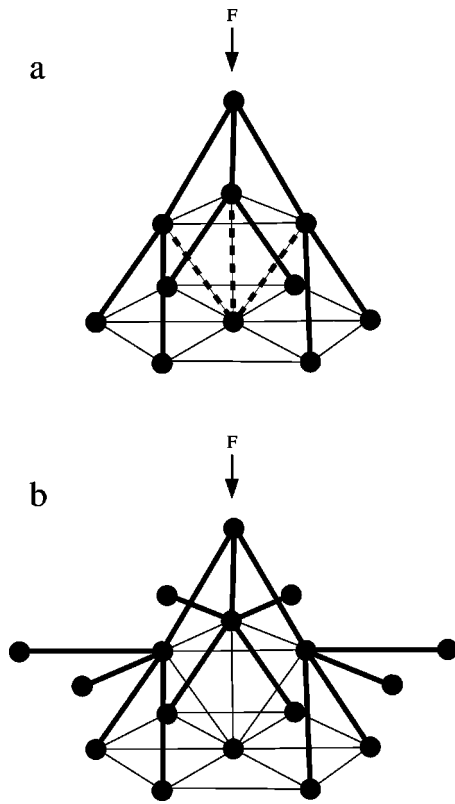


FIG. 10. Schematic diagrams of a perfect hcp crystal. (a) Forces cannot be transferred from the top to the third layer without having negative forces, shown as dashed lines. When the weight of the particles is neglected this pack is unstable without additional support from the sides. (b) Illustration of force being transferred to in-plane neighbors.

not straight lines of beads downward through the pack, so even in a perfect crystal the force cannot be transferred to a single bead and still preserve vector force balance. Furthermore, the nature of the geometry of the hcp crystal is such that the force on a bead in the second layer received from the top bead cannot be transferred to the three beads below. This would require a negative force (see Fig. 10) or adhesion, which is not present in dry granular systems. The result is that a pack such as that shown in Fig. 10(a) is not stable to an external force when there is no friction and the weight of the individual grains is neglected. If only the weight of the beads is considered then a perfect hcp packing is stable down to five layers after which it develops the same instability. In order to keep the beads from moving there must be additional support. Inside a larger crystal this instability demands that forces are transmitted to in-plane beads for close-packed crystals and that forces are transmitted upwards for nonclose-packed crystals. If forces are allowed to be transmitted to in-plane neighbors then Fig. 10(b) shows the propagation of forces for a small piece of a perfect hcp crystal in response to a downwards force at the top. In-plane forces will continue directly to the walls without additional scattering in a perfect crystal. First-order scattering will result in a spokelike pat-

tern at the top surface similar to that seen in the fcc crystals. The expected pattern at the bottom surface is a ring of maximum force, whose radius grows with additional layers of depth at angles of 19.5° and 35.3° for alternating layers. The solid black line in Fig. 5 shows the expected radius of the ring as a function of depth based on an average angle of 27.4° . As the depth of the pack increases, the interior of the ring also fills in. This process occurs even in a perfect hcp crystal. Disorder has little effect on the pattern of forces on the bottom surface, but does result in a spoke pattern on the top surface, as is seen experimentally in Fig. 7.

V. CONCLUSIONS

We have observed that in the highly ordered regime the response to a localized force is greatly dependent on the structure of the beads within a granular pack. We found distinctly different responses from fcc crystals and hcp crystals, both of which behave differently than amorphous packs. Amorphous packs are found to respond with a large central peak. Fcc crystals respond with three regions of large force at the bottom surface, while hcp crystals show rings of maximum force. These structures can be explained by force balance in the geometry of the crystal. These findings are consistent with the two-dimensional results of Geng and co-workers [20,25].

The texture of a granular pack is crucially important for determining the average pattern of stress transmission, as has been suggested by Rajchenbach [26]. The fcc crystal structure, without disorder, leads to a tripod of force chains that is the dominant feature of the force profiles. Small amounts of disorder create secondary structures at the bottom surface and are responsible for a sixfold spoke pattern of forces at the top surface. The hcp crystal structure does not allow for straight line propagation of forces downward through the pack. Even without disorder the forces must split at every layer.

The splitting of forces within an hcp pack can be viewed in analogy to the force chain splitting model of Bouchaud *et al.* [21]. In a perfect hcp crystal the force splitting is driven by the orientations of neighboring grains and is thus nearly uniform everywhere, in contrast to the force chain splitting model in which randomly placed defects drive forces to split into random angles. Nevertheless, the average response of the system to multiple splittings is found to have similarities across these two systems. The force chain splitting model has been shown to lead to a central minimum of force at the bottom surface in response to a localized force at the top for small packing heights, which is consistent with our observations on hcp crystals of small heights. In two-dimensional simulations of force chain splitting with a small density of defects the response pattern made a transition towards elasticlike behavior with a broad central peak for depths larger than approximately six mean free paths of the force [21]. We find that for three-dimensional hcp crystals larger than approximately ten layers in depth the central minimum of force fills in leading to a broad central peak response. This experimental result in three dimensions with splitting generated uniformly throughout the pack by contact

orientations agrees qualitatively with the predictions of the force chain splitting model simulations in two dimensions where randomly placed defects generate the splitting.

Finally, it is important to note that previous experiments have shown that the crystal structure does not affect $P(F)$, the probability distribution of interparticle contact forces [12]. We conclude that the fluctuations of forces within a single pack are dominated by microscopic details of the granular pack and are not influenced by the arrangement of

the beads. Nevertheless, the average response to a localized force is greatly influenced by this structure.

ACKNOWLEDGMENTS

We would like to thank Adam Marshall, Daniel Blair, Daniel Mueth, and Milica Medved for their assistance with this project. This work was supported by NSF under Grant No. cts0090490 and by the MRSEC Program of the NSF under Grant No. DMR-9808595.

-
- [1] J.-P. Bouchaud, M.E. Cates, and P. Claudin, *J. Phys. I* **5**, 639 (1995).
- [2] J.P. Wittmer, P. Claudin, M.E. Cates, and J.-P. Bouchaud, *Nature (London)* **382**, 336 (1996); J.P. Wittmer, P. Claudin, and M.E. Cates, *J. Phys. I* **7**, 39 (1997).
- [3] S.F. Edwards, *Physica A* **249**, 226 (1998).
- [4] D.A. Head, A.V. Tkachenko, and T.A. Witten, *Eur. Phys. J. E* **6**, 99 (2001).
- [5] C. Goldenberg and I. Goldhirsch, e-print cond-mat/0108297; *Phys. Rev. Lett* (to be published).
- [6] I. Goldhirsch and C. Goldenberg, e-print cond-mat/0201081; *Physica A* (to be published).
- [7] A. Stott and M. E. Cates, Final Year Project, The University of Edinburgh, 1998.
- [8] O. Pouliquen, M. Nicolas, and P.D. Weidman, *Phys. Rev. Lett.* **79**, 3640 (1997).
- [9] L. Vanel, A.D. Rosato, and R.N. Dave, *Phys. Rev. Lett.* **78**, 1255 (1997).
- [10] D.G. Scott, *J. Chem. Phys.* **40**, 611 (1964).
- [11] T.G. Owe Berg, R.L. McDonald, and R.J. Trainor, Jr., *Powder Technol.* **3**, 183 (1969).
- [12] D.L. Blair, N.W. Mueggenburg, A.H. Marshall, H. Jaeger, and S. Nagel, *Phys. Rev. E* **63**, 041304 (2001).
- [13] D.M. Mueth, H.M. Jaeger, and S.R. Nagel, *Phys. Rev. E* **57**, 3164 (1998).
- [14] H.A. Makse, D.L. Johnson, and L.M. Schwartz, *Phys. Rev. Lett.* **84**, 4160 (2000).
- [15] G. Løvøll, K.N. Måløy, and E.G. Flekkøy, *Phys. Rev. E* **60**, 5872 (1999).
- [16] M. DaSilva and J. Rajchenbach, *Nature (London)* **406**, 6797 (2000).
- [17] C.-h. Liu, S.R. Nagel, D.A. Schecter, S.N. Coppersmith, S. Majumdar, O. Narayan, and T.A. Witten, *Science* **269**, 513 (1995).
- [18] S.N. Coppersmith, C. Liu, S. Majumdar, O. Narayan, and T.A. Witten, *Phys. Rev. E* **53**, 4673 (1996).
- [19] G. Reydellet and E. Clément, *Phys. Rev. Lett.* **86**, 3308 (2001).
- [20] J. Geng, D. Howell, E. Longhi, R. Behringer, G. Reydellet, L. Vanel, E. Clement, and S. Luding, *Phys. Rev. Lett.* **87**, 035506 (2001).
- [21] J. Bouchaud, P. Claudin, D. Levine, and M. Otto, *Eur. Phys. J. E*, **4**, 4 (2001).
- [22] M.E. Cates, J.P. Wittmer, J.-P. Bouchaud, and P. Claudin, *Phys. Rev. Lett.* **81**, 1841 (1998).
- [23] F. Delyon, D. Dufresne, and Y.-E. Lévy, *Ann. Ponts Chaussees* **22** (1990).
- [24] We used Super Nu-Kote SNK-11 1/2 carbon paper and Hammermill laser print long grain radiant white paper.
- [25] R. Behringer and J. Geng (private communication).
- [26] J. Rajchenbach, *Phys. Rev. E* **63**, 4 (2001).